

Electron Crystallography

Ed. by D. L. Dorset, S. Hovmöller & X. Zou

Kluwer Academic Publishes, The Netherlands, 1998, pp. 285-294.

MULTI-DIMENSIONAL ELECTRON CRYSTALLOGRAPHY OF
Bi-BASED SUPERCONDUCTORS

FAN HAI-FU ^a, WAN ZHENG-HUA ^b, LI JIAN-QI ^c, FU ZHENG-QING ^a,
MO YOU-DE ^a, LI YANG ^a, SHA BING-DONG ^a, CHENG TING-ZHU ^d,
LI FANG-HUA ^a and ZHAO ZHONG-XIAN ^c

^a *Institute of Physics, Chinese Academy of Sciences, Beijing, China*

^b *Department of Physics, Zhongshan University, Guangzhou, China*

^c *National Laboratory for Superconductivity, Chinese Academy of Sciences,
Beijing, China*

^d *Laboratory of Structure Analysis, University of Science and Technology of
China, Hefei, China*

1. Introduction

For the structure analysis of crystalline materials, electron crystallographic methods are in some cases superior to X-ray methods. First, many crystalline materials important in science and technology, such as high T_c superconductors, are too small in grain size and too imperfect in periodicity for an X-ray single crystal analysis to be carried out, but they are suitable for electron microscopic observation. Secondly the atomic scattering factors for electrons differ greatly from those for X-rays and it is easier for electron diffraction to observe light atoms in the presence of heavy atoms (see *figure 1*). Finally the electron microscope is the only instrument that can produce simultaneously for a crystalline sample a micrograph and a diffraction pattern corresponding to atomic resolution. In principle either the electron micrograph (EM) or the electron diffraction (ED) pattern could lead to a structure image. However the combination of the two will make the procedure much more efficient and powerful [1].

The widespread occurrence of incommensurate modulations in the high- T_c superconducting phases and related compounds requires the multi-dimensional crystallographic methods [2] for their structure analysis. On the other hand, the modulation in the high- T_c superconductors involves both the metal and the oxygen atoms. The modulation of the latter in the Bi-O layer is important for understanding the mechanism of superconductivity, since it plays an important role in the incorporation of extra O atoms in the Bi-O layer and hence contributes to the hole concentration in the Cu-O layer. Owing to the dominating effect of heavy atoms in X-ray diffraction, electron diffraction may be a better technique to study the oxygen modulation.

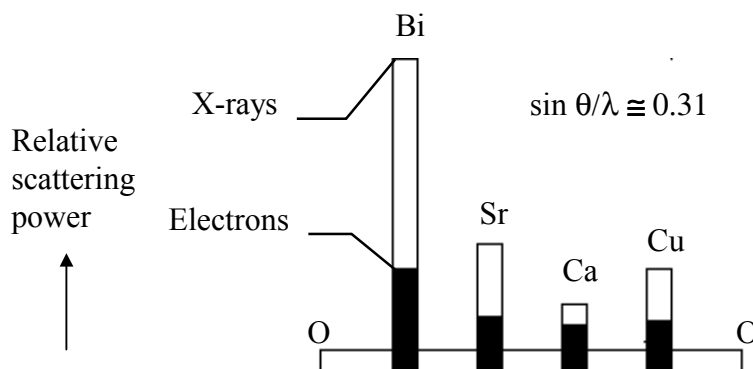


Figure 1. Comparison of the relative scattering power of the elements Bi, Sr, Ca, Cu and O for X-rays and for electrons. Assuming that the relative scattering power of oxygen is the same for X-rays and for electrons, the ratio of relative scattering power between Bi and O is much higher for X-rays (shown as white vertical bar) than for electrons (shown as black vertical bar).

2. The incommensurate modulation in Bi-based superconductors

The chemical formula of the Bi-cuprates can be expressed as $\text{Bi}_2\text{Sr}_2\text{Ca}_{n-1}\text{Cu}_n\text{O}_{2n+4}$ with $n = 1, 2$ and 3 corresponding respectively to the Bi-2201, Bi-2212 and Bi-2223 superconducting phases. The basic structure of these compounds can be regarded as consist of alternately a bismuth-oxygen bi-layer and a perovskite layer as shown schematically in *figure 2*. Electron microscopic studies [3, 4] found that there exist various kinds of incommensurate modulations in the structure of Bi-cuprates (shown schematically in *figure 3*). However with the conventional electron microscopic technique it is difficult to observe the modulated structure at atomic resolution. The superconducting phase Bi-2212 has been extensively studied by X-ray and neutron diffraction methods (see [2] and the references there in). The Bi-2201 phase has also been studied by similar methods [5, 6]. However, the published results are not completely consistent with each other, especially on the oxygen atoms of the Bi-O layer. The Bi-2223 superconductor has the highest T_c value in the Bi-cuprate family. On the other hand it is most difficult to prepare good-quality single crystals suitable for X-ray analysis for this compound. Hence so far there are no reports on single-crystal structure studies of the Bi-2223 phase by either X-ray or neutron diffraction. Finally an important problem in the study of superconductivity is: whether and how the structure of a superconductor changes when the temperature passes through the T_c ? The multidimensional electron crystallographic methods have been used for solving the above problems.

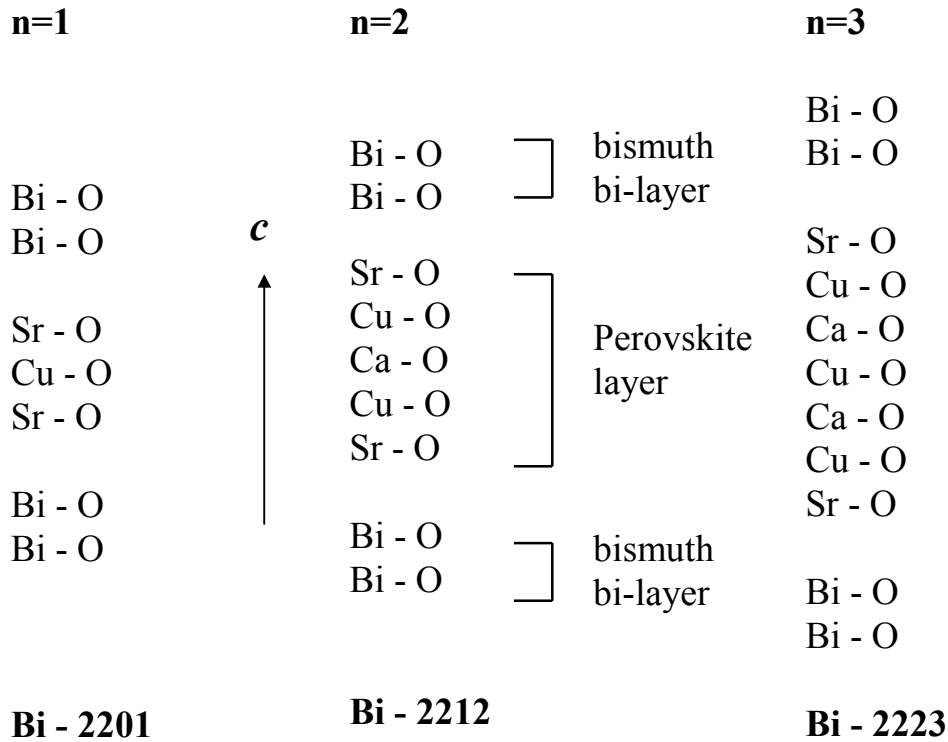
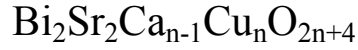


Figure 2. Structure types in the Bi-cuprate family.

2.1. THE INCOMMENSURATE MODULATION OF THE Pb-DOPED Bi-2223 SUPERCONDUCTING PHASE [7]

This work was based on the preliminary electron diffraction study of Li *et al.* [8] and the average structure obtained by Sequeira *et al.* [9]. The diffraction intensities used in our study were measured from the electron diffraction pattern normal to the *a* axis. Since the *a* axis is rather short (5.49Å) and is perpendicular to the modulation vector *q*, no attempt to use 3-dimensional diffraction data was made. The symmetry of the sample belongs to the superspace group P [B bmb] 1-11 with the 3-dimensional unit cell *a* = 5.49, *b* = 5.41, *c* = 37.1Å; $\alpha = \beta = \gamma = 90^\circ$ and the modulation vector $q = 0.117b^*$. Five photographs were taken with different exposure times for the same *oklm* electron diffraction pattern. This is an analogue of the multifold method in X-ray

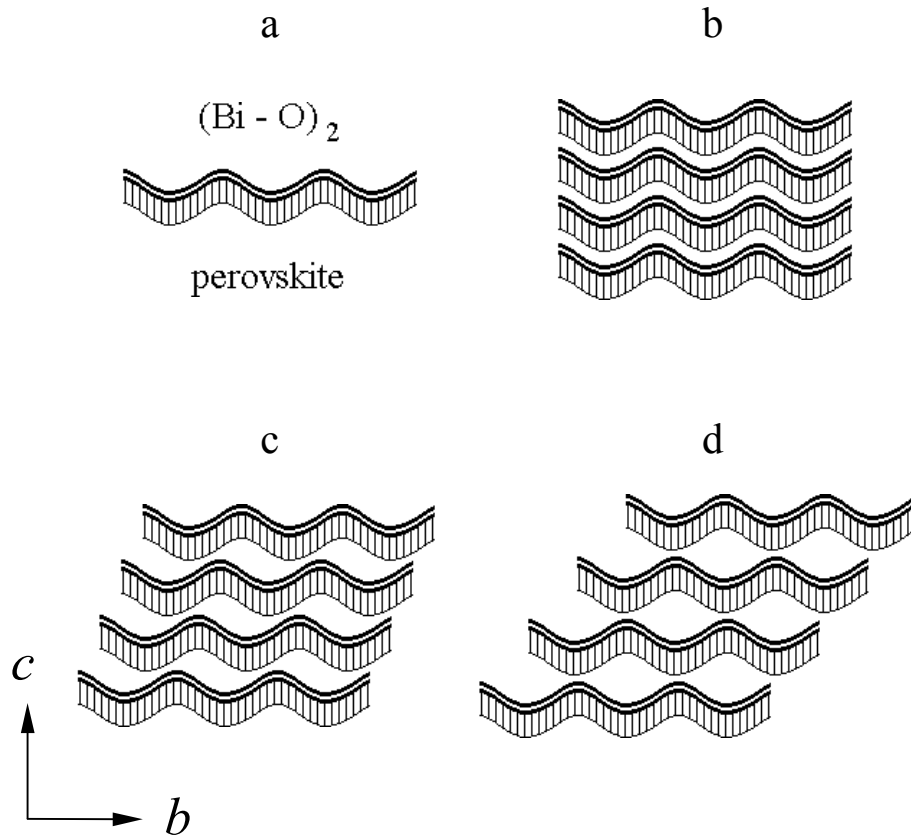


Figure 3. Different modulation modes in the Bi-cuprate family revealed by electron microscopic observation

crystallography for collecting diffraction intensities. A microdensitometer was used to measure the integrated intensities. Structure factor magnitudes were obtained as the square root of diffraction intensities. The R factor for the discrepancy of symmetrically related reflections is 0.12 for the 42 main reflections and 0.13 for the 70 first-order satellite reflections. A few second-order satellites were also observed; however, they are much weaker than the first-order ones and were neglected in the structure analysis.

The structure analysis was carried out in 4-dimensional space, in which the real and the reciprocal unit cells are defined respectively as

$$a_1 = a, \quad a_2 = b - 0.117d, \quad a_3 = c, \quad a_4 = d$$

and

$$b_1 = a^*, \quad b_2 = b^*, \quad b_3 = c^*, \quad b_4 = 0.117 b^* + d$$

where \mathbf{d} is the unit vector normal to the 3-dimensional space, i.e. a unit vector simultaneously perpendicular to the vectors \mathbf{a} , \mathbf{b} , \mathbf{c} , \mathbf{a}^* , \mathbf{b}^* and \mathbf{c}^* . An atom in the 4-dimensional space without modulation will be something like an infinite straight bar parallel to the fourth dimension \mathbf{a}_4 . Occupational modulation will change periodically the width, while positional modulation will change periodically the direction of the bar. Our task is to find out such a periodic change. This can be accomplished by solving the phase problem and calculating the 4-dimensional potential distribution, the 4-dimensional Fourier map. The incommensurate modulated structure in the 3-dimensional physical space can be obtained by cutting the 4-dimensional Fourier map with a 3-dimensional hyperplane perpendicular to the direction \mathbf{a}_4 . While the modulation wave of all the atoms can be measured directly on the 4-dimensional Fourier map. For details of the multidimensional representation of incommensurate modulated structures the reader is referred to the original papers [10-13].

The phases of the main reflections $0kl0$ were calculated from the known average structure. While phases of the satellites $0klm$ were derived by the multidimensional direct method [2]. A Fourier map in multidimensional space was then calculated, from which modulation waves of all metal atoms were measured directly. On this basis least-square refinement ended at an R -factor of 0.16 for the main and 0.17 for the first-order satellite reflections. *Figure 4* shows the modulation waves of the metal atoms. *Figure 5* shows the incommensurate modulation of the Pb-doped Bi-2223 phase in the 3-dimensional physical space projected along the \mathbf{a} axis.

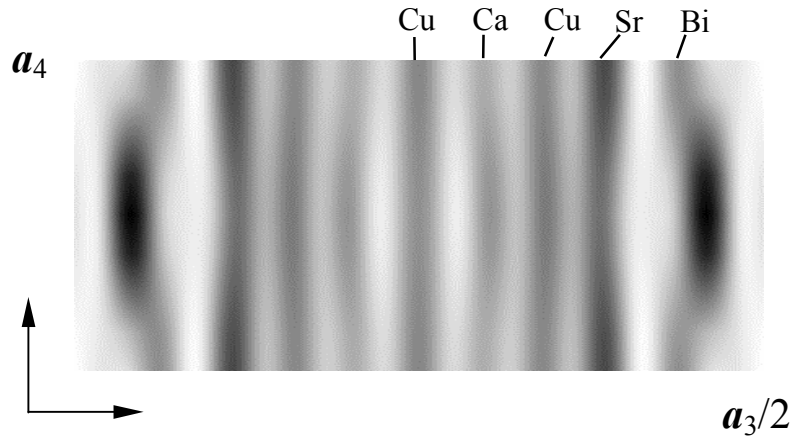


Figure 4. A section, $\int \varphi(x_1, 0, x_3, x_4) dx_1$, of the 4-dimensional Fourier map of the Pb-doped Bi-2223 superconductor projected along the \mathbf{a} axis

As is seen, both occupational and positional modulations are evident for most metal atoms. An other prominent feature is that the oxygen atoms on the Cu-O layers move towards the Ca layer, forming a disordered oxygen bridge across the layers of Cu(2)-Ca-Cu(1)-Ca-Cu(2) (see *figure 5*).

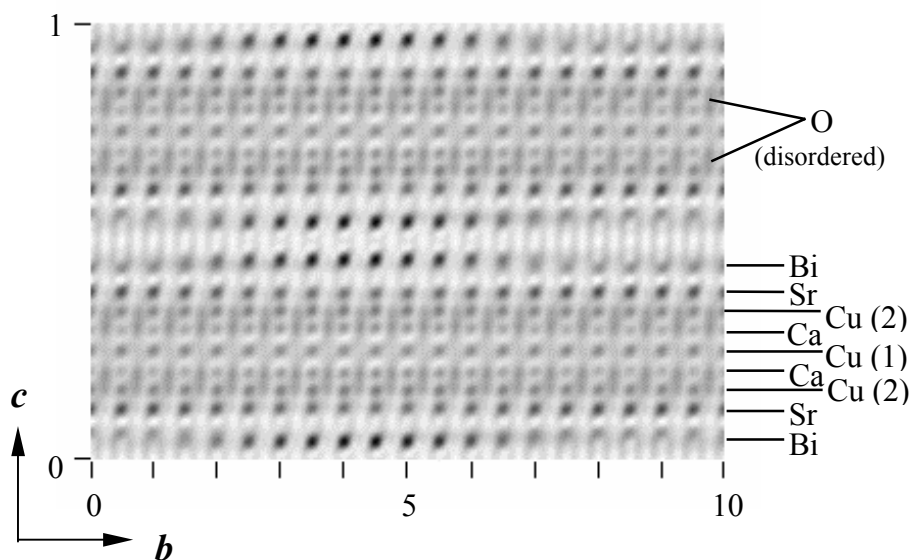


Figure 5. The 3-dimensional potential distribution function of the Pb-doped Bi-2223 superconductor projected along the a axis. Ten unit cells are plotted along the b axis, showing the period of modulation to be approximately 8.5 times the length of b .

2.2. THE INCOMMENSURATE MODULATION OF THE Bi-2212 PHASE [14]

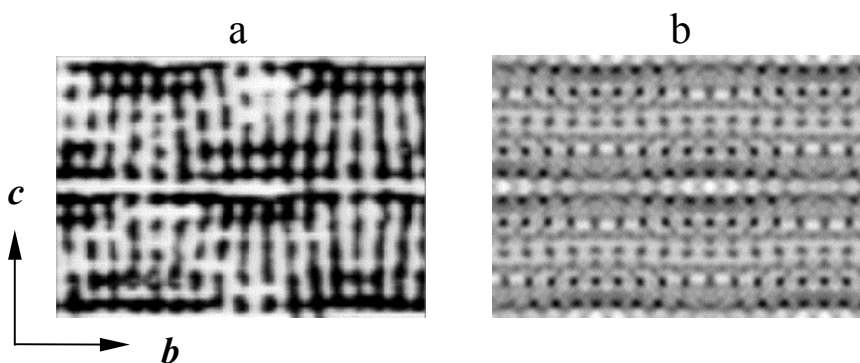


Figure 6. The modulation of the Bi-2212 superconducting phase. (a) experimental EM taken with the incident electron beam parallel with the a axis [3]; (b) the 3-dimensional potential distribution projected along the a axis, calculated using structure-factor magnitudes from the corresponding ED and phases from the EM and the direct-method phase extension.

The superconducting phase Bi-2212 has been extensively studied as described in

reference [2]. However no electron crystallographic methods at atomic resolution were used in the previous studies. We provide here such an example and show how the combination of EM and ED can be used to determine the incommensurate structure even assuming the average structure is unknown. The sample belongs to the superspace group $N [B bmb] 1 -1 1$ with $a = 5.42$, $b = 5.44$, $c = 30.5 \text{ \AA}$, $\alpha = \beta = \gamma = 90^\circ$ and the modulation wave vector $\mathbf{q} = 0.22 \mathbf{b}^* + \mathbf{c}^*$. We started with an EM at 2 \AA resolution (*figure 6a*) and the corresponding ED at 1 \AA resolution. A set of structure-factor magnitudes with indices $0klm$ was measured from the ED. The phases of the main reflections within 2 \AA resolution were obtained from the Fourier transform of the deconvoluted EM. While phases of satellite reflections and of the main reflection beyond 2 \AA resolution were derived by the direct-method phase extension. Finally a Fourier map was calculated (*figure 6b*) which reveals the incommensurate modulation of the structure. This procedure can be regarded as an image processing technique in HREM [1] applied to *figure 6a* by making use of the information from the corresponding ED.

2.3. THE INCOMMENSURATE MODULATION OF THE Bi-2201 PHASE

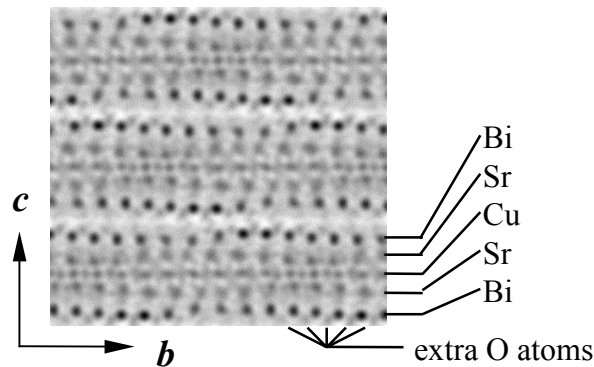


Figure 7. Three-dimensional potential distribution of the Bi-2201 phase projected along the a axis, showing the incommensurate modulation and extra oxygen atoms.

Crystals of Bi-2201 belong to the superspace group $P [B 2/b] -11$ with $a = 5.41$, $b = 5.43$, $c = 24.6 \text{ \AA}$, $\alpha = \beta = \gamma = 90^\circ$ and the modulation wave vector $\mathbf{q} = 0.217 \mathbf{b}^* + 0.62 \mathbf{c}^*$. The structure analysis was based on the known average structure [5]. Only electron diffraction intensities of the $0klm$ reflections were used. Since inconsistent results have been reported on the oxygen atoms [5, 6], special care was taken for their determination. The 4-dimensional Fourier map projected along the a axis was calculated with phases from the average structure and the direct-method phase extension. Apart from two oxygen atoms, which are overlapped with metal atoms respectively on the Bi-O and Sr-O layers, the modulation waves of all symmetrically independent atoms were measured directly from this Fourier map. Up to the fourth-order

harmonics were included in the expression of the modulation function. Fourier recycling and least-squares refinement led to the R factors: $R_T = 0.32$, $R_M = 0.29$, $R_{S1} = 0.29$, $R_{S2} = 0.36$ and $R_{S3} = 0.52$. Here the R factor is defined as $R = \frac{\sum |F_o| - |F_c|}{\sum |F_o|}$, R_T denotes the R factor for the total reflections, R_M for the main reflections, R_{S1} , R_{S2} and R_{S3} respectively for the first-order, second-order and third-order satellite reflections. The resulting Fourier map clearly shows the main feature of the modulation. However, it contains a number of small additional peaks near some of the Bi and Sr sites. After we failed to eliminate them, they were treated as extra oxygen atoms. By including extra oxygen atoms in the Bi-O layer, after a few cycles of refinement, the R factors dropped to 0.23, 0.20, 0.24, 0.27 and 0.30 for R_T , R_M , R_{S1} , R_{S2} and R_{S3} respectively. Further inclusion of extra oxygen atoms in the Sr-O layer, the least-square refinement ended at the R factors of 0.18, 0.13, 0.19, 0.25 and 0.26 for R_T , R_M , R_{S1} , R_{S2} and R_{S3} respectively. *figure 7* is the final Fourier map..

2.4 THE INCOMMENSURATE MODULATION OF THE Bi-2212 PHASE AT THE TEMPERATURES ABOVE AND BELOW T_c

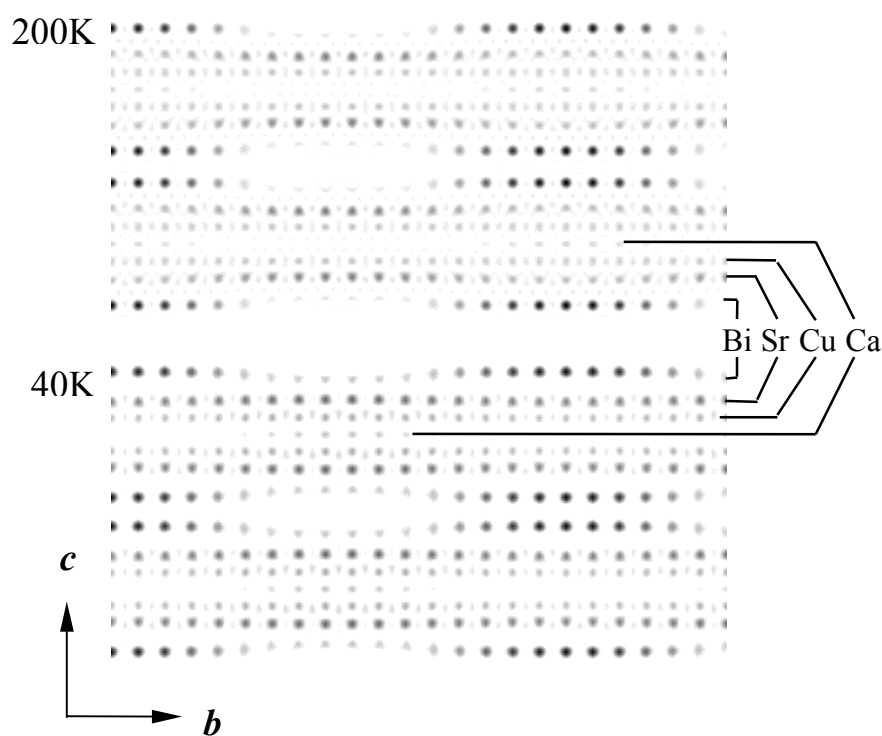


Figure 8. Three-dimensional potential distribution function of the Bi-2212 phase projected along the a axis. Upper: at the temperature above T_c ; Lower: at the

temperature below T_c .

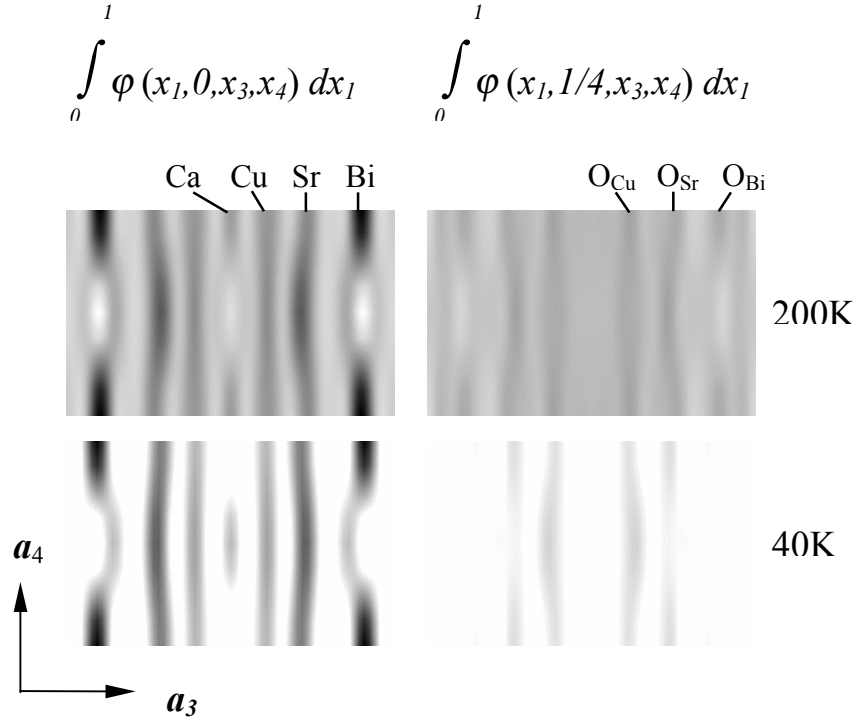


Figure 9. Sections of the 4-dimensional Fourier map of the Bi-2212 phase projected along the a axis. Upper: at the temperature above T_c ; Lower: at the temperature below T_c . Left: sections showing the metal atoms; Right: sections showing oxygen atoms near $x_2 = 1/4$.

The sample belongs to the superspace group P [B bmb] 1 -1 1 with $a = 5.40$, $b = 5.38$, $c = 30.80\text{\AA}$; $\alpha = \beta = \gamma = 90^\circ$ and the modulation vector $\mathbf{q} = 0.117\mathbf{b}^*$. Note that the modulation mode of this sample is different with that of the Bi-2212 sample described in Section 2.2. Electron diffraction patterns were taken respectively at the temperature of 200K (above T_c) and 40K (below T_c) and with the incident electron beam parallel to the a axis. The multidimensional direct method was used to determine the incommensurate modulation.

Figure 8 shows the resultant 3-dimensional potential distribution projected along the a axis. figure 9 shows Fourier hyper-sections through the average position of the metal atoms and the overlapped oxygen atoms. As is seen, the variations of atoms in both occupancy and position are on average weaker at 40K (below T_c) than that at 200K (above T_c). A prominent feature can be seen in figure 8 is that the modulation wave of the Ca atoms shifts one half of its period along the b direction. Another prominent, and

perhaps more important, feature in *figure 9* is that the ‘extra’ oxygen atoms, which distribute on the Bi-O, Sr-O and Cu-O layers at 200K, move towards the Cu-O layer at the temperature below T_c (40K).

References

1. Li, F. H. (1997) Image restoration - crystal structure determination by image deconvolution and resolution enhancement, (in this *Proceedings*).
2. Fan, H. F. (1997) Multi-dimensional direct methods, (in this *Proceedings*).
3. Matsui, Y. and Horiuchi, S. (1988) Geometrical relations of various modulated structures in Bi-Sr-Ca-Cu-O Superconductors and related compounds, *Jpn. J. Appl. Phys.* **27**, L2306-L2309.
4. Ikeda, S., Aota, K., Hatano, T. and Ogawa, K. (1988) A new mode of modulation observed in the Bi-Sr-Ca-Cu-O system, *Jpn. J. Appl. Phys.* **27**, L2040-L2043.
5. Gao, Y., Lee, P., Ye, J., Bush, P., Petricek, V. and Coppens, P. (1989) The incommensurate modulation in the $\text{Bi}_2\text{Sr}_{2-x}\text{Ca}_x\text{Cu}_2\text{O}_6$ superconductor, and its relation to the modulation in $\text{Bi}_2\text{Sr}_{2-x}\text{Ca}_x\text{Cu}_2\text{O}_8$, *Physica C* **160**, 431-438.
6. Yamamoto, A., Takayama-Muromachi, E., Izumi, F., Ishigaki, T. and Asano, H. (1992) Rietveld analysis of the composite crystal in superconducting $\text{Bi}_{2+x}\text{Sr}_{2-x}\text{CuO}_{6+y}$, *Physica C* **201**, 137-144.
7. Mo, Y. D., Cheng, T. Z., Fan, H. F., Li, J. Q., Sha, B. D., Zheng, C. D., Li, F. H. and Zhao, Z. X. (1992) Structural features of the incommensurate modulation in the Pb-doped Bi-2223 high T_c phase revealed by direct-method electron diffraction analysis, *Supercond. Sci. Technol.* **5**, 69-72.
8. Li, J. Q., Yang, D. Y., Li, F. H., Zhou, P., Zheng, D. N., Ni, Y. M., Jia, S. L. and Zhao, Z. X. (1989) Structure Symmetry and microstructures of Bi(Pb)-Sr-Ca-Cu-O system, *Progress in High T_c Superconductivity* **22**, 441-443.
9. Sequeira, A., Yakhmi, J. V., Iyer, R. M., Rajagopal, H. and Sastry, P. V. P. S. S. (1990) Novel structural features of Pb-stabilised Bi-2223 high- T_c phase from neutron-diffraction study, *Physica Scripta C* **167**, 291-296.
10. Janner, A. and Janssen, T. (1977) Symmetry of periodically distorted crystals, *Phys. Rev. B* **15**, 643-658.
11. De Wolff, P. M. Janssen, T. and Janner, A. (1981) The superspace groups for incommensurate crystal structures with a one-dimensional modulation, *Acta Cryst.* **A37**, 625-636.
12. Janner, A. Janssen, T. and De Wolff, P. M. (1983) Bravais classes for incommensurate crystal phases, *Acta Cryst.* **A39**, 658-666.
13. Jansen, T., Janner, A., Looijenga-Vos, A. and De Wolff, P. M. (1992) Incommensurate and commensurate modulated structures, in Wilson, A. J. C. (ed.), *International Tables for Crystallography*, Kluwer Academic Publishers, Dordrecht, pp. 797-835; 843-844.
14. Fu, Z. Q., Huang, D. X., Li, F. H., Li, J. Q., Zhao, Z. X., Cheng, T. Z. and Fan, F. F. (1994) Incommensurate modulation in minute crystals revealed by combining high-resolution electron microscopy and electron diffraction, *Ultramicroscopy* **54**, 229-236.